npj biofilms and microbiomes

www.nature.com/npjbiofilms

BRIEF COMMUNICATION OPEN

Check for updates

Ex vivo intestinal permeability assay (X-IPA) for tracking barrier function dynamics

Hadar Bootz-Maoz[1,2], Ariel Simon[1,2], Sara Del Mare-Roumani[1,2], Yifat Bennet[1,2], Einat Toister[1,2], Hadar Romano[1,2], Danping Zheng[3], Sivan Amidror[1,2], Eran Elinav[3,4] and Nissan Yissachar[1,2]✉

The intestinal epithelial barrier facilitates homeostatic host–microbiota interactions and immunological tolerance. However, mechanistic dissections of barrier dynamics following luminal stimulation pose a substantial challenge. Here, we describe an ex vivo intestinal permeability assay, X-IPA, for quantitative analysis of gut permeability dynamics at the whole-tissue level. We demonstrate that specific gut microbes and metabolites induce rapid, dose-dependent increases to gut permeability, thus providing a powerful approach for precise investigation of barrier functions.

npj Biofilms and Microbiomes (2023)9:44 ; https://doi.org/10.1038/s41522-023-00409-0

The gut microbiota is confined to the lumen by a single layer of intestinal epithelial cells (IECs). Continuous replenishment of the IEC layer by Lgr5+ intestinal stem cells and physical reinforcement by inter-epithelial tight-junction (TJ) proteins are crucial to maintain barrier integrity and tissue homeostasis[1]. Interference with epithelial barrier integrity (e.g., by pathogenic microbes or drugs) leads to enhanced gut permeability and enables translocation of previously confined (and potentially harmful) microorganisms into the tissue and to distal locations including secondary lymph nodes and liver, where they trigger inflammatory responses[2–4]. Indeed, disruptions to epithelial barrier functions and a 'leaky gut' are implicated in both intestinal and extraintestinal pathologies, including allergic and autoimmune conditions, inflammatory bowel diseases, irritable bowel syndrome and cancer[5].

Existing methods for evaluation of epithelial barrier functions and gut permeability include trans-epithelial electrical resistance (TEER) assay, measurement of ion transport in an Ussing chamber, and oral gavage of animal models with fluorescently labeled molecules followed by quantification of serum fluorescence[6]. However, these approaches do not support real-time perturbations and readouts in an intact, whole-tissue setting, and thus do not provide temporal information of barrier dynamics.

To finely dissect host-microbiota interactions, we developed a unique gut organ culture system that maintains the naïve intestinal tissue architecture and provides tight experimental control[7]. We have demonstrated that this system is ideal for investigating rapid intestinal responses to specific bacterial strains[7], whole human microbiota samples[8,9], drugs and metabolites[10]. The emerging realization that the gut microbiota and its associated metabolites regulate intestinal barrier functions[10–12] drove us to investigate whether the advantages of the gut organ culture system could be harnessed to uncover mechanisms underlying microbial regulation of gut permeability.

Here, we aimed to measure rapid and subtle changes to gut permeability following luminal stimulation, in multiple gut tissues, under tightly controlled experimental conditions and in high temporal resolution. We developed and optimized an ex vivo intestinal permeability assay (X-IPA) in which fluorescein isothiocyanate (FITC)-dextran is infused directly into the lumen of the cultured gut tissues (Fig. 1A). Migration of luminal FITC-dextran to the extraintestinal culture medium depends on integrity of the epithelial barrier. Thus, fluorescence intensity of the extraintestinal medium corresponds with epithelial barrier integrity and permeability.

In a set of proof-of-principle experiments, we measured gut permeability ex vivo in response to luminal introduction of EGTA, a calcium chelator that disrupts TJ integrity and paracellular barrier functions (confirmed using dynamic TEER assay (Fig. 1B, C) and ZO-1 staining (Fig. S1A) in Caco-2 monolayers). Colon tissues were dissected from 14d-old mice reared under specific-pathogen-free (SPF) conditions, and connected to the gut culture device as previously described (six tissues per device; Fig. 1A)[7,8,13]. Culture medium containing FITC-dextran (4 kDa) was infused directly into the cultured colons' lumens either with or without EGTA (25 mM). Compared with controls, luminal EGTA infusion disrupted epithelial barrier integrity, as indicated by marked decreases in ZO-1 TJ protein expression (Fig. 1D, E). In agreement, luminal infusion of EGTA resulted in rapid and significant increase in extraintestinal FITC-dextran throughout the experiment (2 h, 8 h), compared with internal controls (Fig. 1F), supporting the utility of the X-IPA system in evaluating changes to gut permeability.

We next asked whether EGTA-induced barrier loss observed in Fig. 1F is attributed to increased TJ-controlled paracellular permeability (leak pathway) or to non-specific epithelial damage (unrestricted pathway). To address this question, we used 70 kDa FITC-dextran, a larger molecule that can cross the barrier only in an unrestricted manner (in contrast to 4 kDa FITC-dextran which can pass via increased paracellular permeability[14]). Interestingly, luminal infusion of EGTA and 70 kDa FITC-dextran did not increase extraintestinal medium fluorescence (Fig. 1G and Fig. S1D), suggesting that the X-IPA system maintains the viability and functional integrity of the epithelial barrier, and may be used to detect changes in TJ-controlled paracellular permeability.

A major advantage of the gut organ culture system is the ability to track rapid intestinal responses to experimental perturbations, over time. To quantify barrier dynamics, we added three upright fluorescence digital microscopes (Dino-Lite) to the gut culture

[1]The Goodman Faculty of Life Sciences, Bar-Ilan University, Ramat-Gan 5290002, Israel. [2]Bar-Ilan Institute of Nanotechnology and Advanced Materials, Bar-Ilan University, Ramat-Gan 5290002, Israel. [3]Systems Immunology Department, Weizmann Institute of Science, 234 Herzl Street, Rehovot 7610001, Israel. [4]Microbiome & Cancer Division, Deutsches Krebsforschungszentrum (DKFZ), Neuenheimer Feld 280, 69120 Heidelberg, Germany. ✉email: nissan.yissachar@biu.ac.il

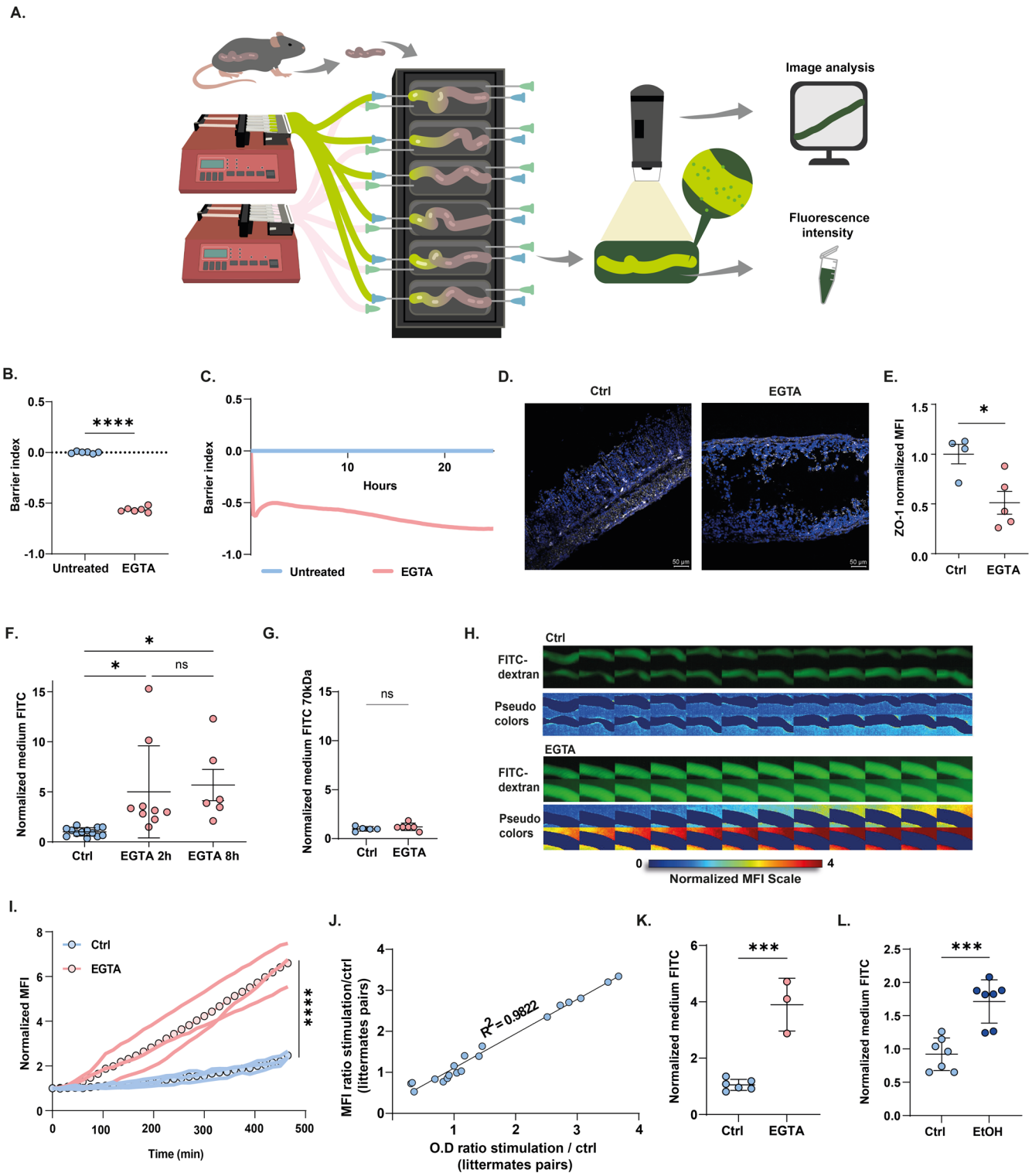

system setup, where each microscope tracks two cultured gut fragments (Fig. 1A). Using this set-up, we could efficiently detect subtle changes in medium concentrations of FITC-dextran by quantifying mean fluorescence intensity (MFI) measurements (dynamic range: 1–100 µg/mL; Fig. S1B).

We acquired time-lapse movies of gut organ cultures following luminal introduction of EGTA, at a temporal resolution of 5 min (for 2 h experiments) or 15 min (for 8 h experiments) (Fig. 1H, I and Supplementary Video 1). For automated analysis and quantification, we developed a MATLAB-based image analysis tool and user-friendly interface (X-IPA analyzer; Fig. S1C and extended data). This software allowed us to generate dozens of single-tissues time traces and quantify extraintestinal medium MFI, for accurate and comparable characterization of gut permeability dynamics in multiple tissues, over time (Fig. 1I). Automated analysis of time-lapse movies revealed a slow and continuous increase in extraintestinal MFI in non-stimulated tissues (average slope $m = 0.17$), which we interpret as steady-

Fig. 1 Development of an ex vivo intestinal permeability assay (X-IPA). A Intact intestinal mice tissues are connected to the gut organ culture device and FITC-dextran is infused into the gut lumen. Diffusion over time is quantified by fluorescence intensity of the extra-intestinal medium (time-lapse imaging) and at the experiment end-point (fluorometer), as an indicator of gut permeability degree and temporal dynamics. **B**, **C** Normalized TEER values for Caco-2 cells supplemented with EGTA after 8 h (**B**) and versus time (**C**). **D**, **E** Confocal imaging of colon segments cultured for 8 h, immuno-stained for ZO-1 (white; DAPI nuclear stain in blue) (**D**) and quantification of ZO-1 MFI following EGTA infusion ($p = 0.03$) (**E**). **F** Normalized extraintestinal medium fluorescence of colon cultures infused with 4kDa-FITC-dextran, with or without EGTA, at 2 h ($p = 0.02$) and 8 h ($p = 0.04$). **G** Normalized extraintestinal medium fluorescence in colon cultures infused with 70kDa-FITC-dextran, with or without EGTA at 4 h. **H** Filmstrips showing gut organ cultures infused with FITC-dextran only (Ctrl) or together with EGTA. The pseudo-color imaging illustrates MFI quantification of FITC-dextran concentrations in the extraintestinal medium. Frames are separated by 15 min. Tissue dimensions captured = ~2 cm **I** Single colon time traces showing normalized MFI of the extraintestinal medium in tissues infused with EGTA or sterile medium (Ctrl). Circles represent average permeability rates. **J** MFI and medium fluorescence intensity (O.D) are tightly correlated ($R^2 = 0.9822$). **K** Normalized extraintestinal medium fluorescence of small intestinal organ cultures infused with EGTA or sterile medium (Ctrl) at 4 h ($p = 0.0001$). **L** Normalized extraintestinal medium fluorescence of colon cultures infused with 5% EtOH or sterile medium (Ctrl) at 4 h ($p = 0.0033$). Statistical significance between two groups was determined by Student's *t* test, or by one-way ANOVA (for three or more independent groups), *p* values: ****<0.0001; ***<0.001; **<0.01; ns not significant. For all panels, mean and standard deviation is shown.

state gut permeability rate under culture conditions. In contrast, EGTA-infused tissues displayed a rapid increase in extraintestinal MFI (average slope $m = 0.75$), observed already at 2 h post-stimulation (Fig. 1I and Supplementary Video 1). We analyzed FITC-dextran spatial distribution along each intestinal fragment to validate tissue integrity and to exclude potential leaking of FITC-dextran from the input or output ports (Supplementary Fig. 2A). Further, medium fluorescence at the experiment endpoint (measured by fluorometer) and corresponding image MFI (calculated by image analysis) were well correlated ($R^2 = 0.9822$), demonstrating that time-lapse imaging and analysis can reliably track and quantify gut permeability dynamics (Fig. 1J).

We further utilized the X-IPA system to track gut permeability dynamics in EGTA-infused small intestinal organ cultures (ileum, Fig. 1K and Supplementary Video 2), and in response to barrier-disrupting ethanol[15] (colon cultures, Fig. 1L, Fig. S1E, and Supplementary Video 3).

Next, to explore whether the X-IPA system could detect changes to gut permeability induced by intestinal metabolites, gut organ cultures were infused with putrescine, a polyamine compound produced by the gut microbiota which we recently identified as a potent disruptor of the intestinal epithelial barrier[10]. At 4 h post-stimulation, we observed a dose-dependent increase in gut permeability in putrescine-infused organ cultures (average slopes: 33 mM $m \approx 0$; 66 mM $m = 0.28$; 100 mM $m = 0.42$), compares with controls (Fig. 2A). Automated image analysis revealed a gradual increase in the FITC-dextran diffusion rate (steeper linear slope) in response to increasing putrescine concentrations (Fig. 2B, C and Supplementary Video 4). These results could support a model in which TJ opening is a continuous process linearly tuned by luminal signal intensity (putrescine concentration) subsequently resulting in increased permeability.

Finally, we sought to examine changes to gut permeability induced by the gut microbiota. We analyzed colonic responses to the anaerobic human commensal *Bifidobacterium adolescentis*, a Th17-inducing microbe[16] which we recently identified as a diet-sensitive pathobiont that alters TJ integrity and disrupts gut barrier functions in vitro and in vivo[9]. We infused medium containing FITC-dextran and equivalent amounts of *B. adolescentis* or *B. fragilis* (an anaerobic human symbiont that does not induce Th17 development[17] nor disrupt the epithelial barrier[9]) into the lumen of colonic organ cultures. We observed an increase in extraintestinal MFI in response to barrier-disrupting *B. adolescentis*, but not to *B. fragilis*, at 4 h post-stimulation (Fig. 2D). In agreement, time-lapse movies revealed that luminal introduction of *B. adolescentis* rapidly increased extraintestinal MFI (average slope $m = 0.22$), while tissues infused with *B. fragilis* were indistinguishable from controls (average slope $m \approx 0$) (Fig. 2E, F and Supplementary Video 5).

Similar results were obtained in response to barrier-disrupting *E. gallinarum*[3], compared with non-disrupting *B. acidifaciens*[18–20] using in vitro TEER assay (Fig. 2G, H) and the X-IPA system (Fig. 2I).

Taken together, we present a unique organ culture-based gut permeability assay. The X-IPA system provides quantitative insights into the effects of luminal perturbations on gut permeability at the whole-tissue level, thus bridging the gap between simplified in vitro assays and complex in vivo animal models. Moreover, this system allows to quantify dynamic behaviors of the intestinal barrier as they occur, over time, in high temporal resolution. We should acknowledge the current limitations of the X-IPA system. In its current setting, the system probably cannot detect transcellular epithelial passage, and is limited to short-term culture (up to 24 h) of tissues dissected from mice (not humans). Additional readouts (including next-generation sequencing, cell sorting, and imaging) applied to the cultured tissues will complement dynamic permeability measurements, thus providing a powerful approach for integrated investigations of host–microbiome interactions.

Given the emerging therapeutic potential of barrier modulating agents, we anticipate that the ability to perturb multiple intestinal tissues and to track subsequent gut barrier functions will further advance mechanistic insights and translational discoveries.

METHODS

Mice

Small and large intestinal tissues used in the ex vivo organ culture system were dissected from sacrificed C57BL/6J (B6) mice. Mice were obtained from Envigo RMS (Israel) and reared in the specific-pathogen-free (SPF) facility at Bar-Ilan University (Israel). For gut organ culture permeability assays, gut tissues were dissected from 14-day-old littermates. All experiments were performed following animal protocol approved by the Bar-Ilan University ethics committee (ethics approval number BIU-BIU-IL-2203-131-1).

Gut organ culture system and X-IPA permeability assay

Fabrication of the gut organ culture device and gut organ culture experiments (Yissachar et al.[7]) were performed with the addition of carbon black (Holland-Moran Cas#1333-86-4) into the PDMS (184 ®SYLGARD#761036) mixture, for fabrication of black, opaque gut culture devices. Briefly, intact whole colons were dissected sterilely from 14-day-old C57BL/6 mouse littermates reared under SPF conditions. The solid lumen content was gently flushed, and the gut fragment was threaded and fixed over the luminal input and output ports of the gut organ culture device, using sterile surgical thread. The culture device was placed in a custom-made incubator that maintains a temperature of 37 °C, and tissue was maintained half-soaked in sterile, serum-free culture medium (Iscove's Modified Dulbecco's Medium without phenol-red (IMDM,

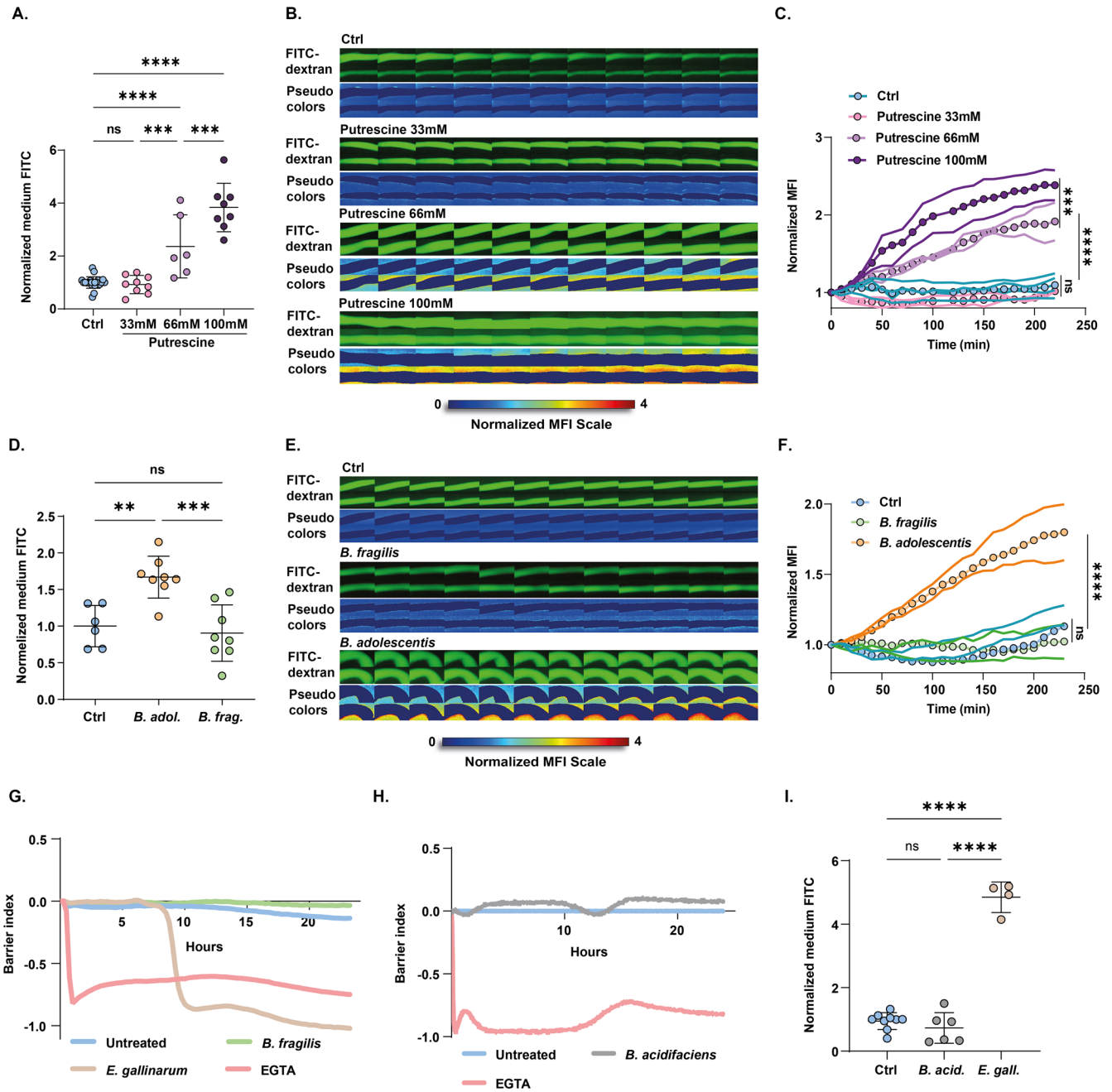

Fig. 2 Rapid modulation of gut permeability by metabolites and gut bacteria. A, **D** Normalized extraintestinal medium fluorescence of gut cultures infused with increasing putrescine concentrations (**A**) or equivalent load of *B. adolescentis* or *B. fragilis* cultures (**D**), at 4 h post-infusion (normalized to internal control). **B**, **E** Filmstrips showing gut organ cultures infused with FITC-dextran only (Ctrl) or with putrescine (**B**) or microbial cultures (**E**). The pseudo-color-imaging illustrates MFI quantification of FITC-dextran concentrations in the extraintestinal medium. Frames are separated by 10 min. **C**, **F** Single colon time traces showing normalized MFI of the extraintestinal medium in tissues infused with putrescine (**C**) or microbial cultures (**F**) and sterile medium (Ctrl). **G**, **H** Normalized TEER values of Caco-2 cells co-cultured with *E. gallinarum* (**G**) or *B. acidifaciens* (**H**), over time. **I** Normalized extraintestinal medium fluorescence of gut cultures infused with *E. gallinarum* ($p < 0.0001$) or *B. acidifaciens*, for 4 h. Statistical significance was determined by one-way ANOVA, *p* values: ****<0.0001; ***<0.001; **<0.01; ns not significant.

GIBCO) supplemented with 20% KnockOut serum replacement (GIBCO), 2% B-27 and 1% of N-2 supplements (GIBCO), 1% L-glutamine, 1% non-essential amino acids, 1% HEPES) using a syringe pump. FITC-dextran (4kD) (0.5 mg/mL; Sigma-Aldrich Cas#60842-46-8) was resuspended in sterile culture medium without phenol-red and infused into the gut lumen using a syringe pump, with or without EGTA (25 mM) (Sigma-Aldrich Cas#13368-13-3), 5% EtOH, purified bacterial cultures (*B. adolescentis*, *B. fragilis*, *E. gallinarum* or *B. acidifaciens* at 10^{7-9} CFU/mL) or putrescine (Sigma, diluted to final concentrations of 33/66/100 mM). Gas outlet in the device lid enabled the flow of a humidified and filtered, medical grade 95% O_2/5% CO_2 gas mixture into the device. Experiments were terminated at 2–8h post-stimulation. A fluorescence video microscope (Dino-Lite, Iner Tech Dino-Capture 2.0 AM4115T-GRFBY) acquired time-lapse movies of the cultured tissues and their surrounding culture medium for downstream image analysis and fluorescence quantification. At the experiment end point, the FITC-dextran

concentration in the extraintestinal medium was determined by quantifying the fluorescence intensity using a fluorometer (excitation 485 nm, emission 520 nm). After culture, tissues were subjected to further analysis (including immunofluorescence staining and imaging).

Image analysis of time-lapse imaging

Software development. Automated computerized image analysis of time-lapse movies was performed with the X-IPA Analyzer, a custom written MATLAB software (created in the MathWorks 2020 platform). The main functions in the software are image pre-processing, tissue segmentation and quantification of the green fluorescence intensity of the extraintestinal medium in each chamber, over time (Supplementary Fig. 1).

Experimental design. The experiments were carried out within an organ culture device that contains six chambers, each containing an intact colon tissue and external medium. Three Dino-Lite microscope cameras were placed over the device, such that each one could capture two chambers. The images were taken at regular intervals of 5 min (for 2 h experiments), 10 min (for 4 h experiments) or 15 min (for 8 h experiments). A series of images per chamber was analyzed.

Analysis algorithm. The algorithm works as follows: The tissue-images are loaded and manually cropped to select pixel-coordinates that represent the measurement area. This area includes the colon-tissue itself and the external tissue-medium. After user-confirmation, the green channel of the RGB model is chosen and the images denoised using a Gaussian filter with a standard deviation of two. The denoised images are segmented by an automated threshold using Otsu's method from Gray-Level Histograms (Binarization), and the tissue segmentation is expanded by an additional 8 pixels in each direction. Per image, the medium pixels (area outside of the segmentation) are measured, and their mean value is calculated. These mean values are shown in a plot, demonstrating MFI (mean fluorescence intensity) changes over time.

The O.D ratio was calculated by dividing the final concentration of the FITC-dextran (μg/mL) by the final concentration of the sterile medium (Ctrl). The MFI ratio was calculated by dividing the value of the FITC-dextran normalized-MFI final value by the sterile medium (Ctrl) normalized-MFI final value.

All steps of analysis can be easily performed with a user-friendly interface (detailed user manual is provided in the online extended data).

Bacterial cultures

B. adolescentis, B. fragilis, and *B. acidifaciens* were obtained from DSMZ (Germany). *E. gallinarum* was kindly provided by Prof. Martin Kriegel (Muenster University, Germany). Bacterial classification was further validated by Sanger sequencing of the 16 S gene. Microbes were incubated overnight in rich liquid medium (2% proteose peptone (Thermo Fisher Cat#LP0085), 0.5% NaCl (Mercury Cat#1064041) and 0.5% yeast extract (Merck Cas#8013-01-2)) supplemented with 250 mg/mL glucose (Mercury Cas#50-99-7), 250 mg/mL K_2HPO_4 (Holland Moran Cas#7758-11-4), 50 mg/mL L-cysteine (Merck Cas#52-90-4), 5 mg/mL Hemin (Mercury Cat#3741) and 5 μL/mL vitamin K_1 (Merck Cas#84-80-0) under anaerobic conditions. *B. acidifaciens* was first incubated in chopped meat medium and then transferred to rich liquid medium.

Cell line

Caco-2 cell line was kindly provided by Professor Ohad Gal Mor (Sheba Medical Center, Israel). Cells were cultured at 37 °C with 5% CO_2 until 80% confluence. For co-culture experiments, Caco-2 cells were cultured with growth media without antibiotics and were seeded on a 24-well plate (at 2×10^5 cells per well). The cells were grown for 4 days and then incubated with 2 mM EGTA, or with purified bacterial cultures resuspended in Caco-2 growth media.

Dynamics trans-epithelial electrical resistance (TEER) measurements

Caco-2 cells were seeded on a CytoView Z, 96-well impedance plate (5×10^5 cells per well) (Axion BioSystems; cat: Z96-IMP-96B-25) and monitored by Maestro Edge platform (Axion BioSystems) until reaching full confluence (800–1200 ohm, usually within 4 days). The barrier index (which represents barrier integrity) was calculated by the Axion "Impedance" module as the ratio between cellular resistance at low frequency (1 kHz) vs. high frequency (41 kHz). For co-culture experiments, microbes were centrifuged at $4200 \times g$ for 10 min and resuspended in 1.5 mL cell culture media without antibiotics. Following serial dilutions, a final volume of 200 μL was added in each well. Microbial load (CFU/mL) was calculated in each experiment. The barrier index was measured at high temporal resolution of 1 min for 24 h and was normalized to the reference time ($t = 0$). An additional correction was performed by normalizing to the barrier index of unstimulated cells.

Immunofluorescence staining of tissue sections, and confocal imaging

For tissue section staining, intestinal tissues were embedded in OCT and stored at −80 °C. The fresh-frozen tissues were sliced using a cryostat (CM1950) into 7 μm sections. The sections were fixed with cold acetone (100%) for 20 min, washed twice in PBS and blocked (10% donkey serum, 0.1% triton in PBS) for 1 h at room temperature. Tissue sections were then stained for ZO-1, diluted 1:100 (Invitrogen Cat 40-2200) overnight at 4 °C. Excess antibody was washed three times and incubated with secondary antibody (Cy3 anti rabbit Jackson-immuno Cat#711-165-152; diluted 1:250) for 1 h at room temperature. After washing, the sections were stained with DAPI (Merck Cat#1246530100). and mounted (fluoroshield) using an antifade reagent (Sigma F6182).

Tissue sections were visualized using a confocal fluorescence microscope (Leica) and processed and analyzed using ImageJ software. To measure the ZO-1 intensity only in the periphery of the intestinal epithelium, an ImageJ macro was employed, using the following workflow: The images were first Gaussian smoothed (sigma = 2), and then segmented by the percentile auto threshold algorithm using the E-cadherin staining. Binary holes were filled to obtain a uniform layer. Next, an ROI (region of interest) band, representing the edge of the intestinal crypt, enclosing the ZO-1 staining, was created as follows: First, the segmented tissue was duplicated and eroded to get a thinner segment. Second, the segmented tissue image was duplicated and dilated to get a wider segment. Finally, the eroded image was subtracted from the dilated image to yield a band, representing the tissue edge. Note, that while the macro allows adjustment of the number of pixels to erode and dilate, once optimal numbers were determined for our images to cover ZO-1, these factors were kept constant for all treatments and for each experiment type. Finally, Analyze Particles was employed to measure the intensity of the total ZO-1 (Cy3) in the ROI.

The intensity of ZO-1 in cultured cells was measured as follows: Smoothing on the ZO-1 image (channel 3 Cy3) using Gaussian blur (sigma = 1) was applied. Next, the background was subtracted (rolling ball = 10). The cells were then segmented using the automatic Otsu algorithm. Finally, the intensity of the ZO-1 marker was calculated according to the binary segmented image.

Immunofluorescence staining of cultured cells

Cells were seeded 4 days pre-treatment on 13 mm coverslips cleaned with 70% EtOH and treated with PDL (0.08 µg/mL) in 24-well plate. Caco-2 cells were then washed with PBS and co-cultured with EGTA (2 mM) for 1 h. Caco-2 cells were fixed and permeabilized (0.5% triton in 3% PFA) for 3 min and then washed with PBS. Then, cells were further fixed (3% PFA) for 30 min, and washed twice with PBS for 10 min. Cells were incubated with blocking solution (10% donkey serum) for 1 h. The cells were then labeled with primary antibody against ZO-1, diluted 1:200 (BD cat:610967) overnight at 4 °C. Excess antibody was washed three times with blocking solution and the cells were incubated with secondary antibody (Cy3 anti mouse, diluted 1:500, Jackson cat: 715-165-151) for 1 h at room temperature. Cells were washed and mounted using fluoro-mount-G. Cells were visualized using a confocal fluorescence microscope (Leica).

Reporting summary

Further information on research design is available in the Nature Research Reporting Summary linked to this article.

DATA AVAILABILITY

All data generated and analyzed in this study are available within the main text and/or the Supplementary Materials. Code and scripts generated in this study are available in the Supplementary Materials. Any additional information that may be required to support the findings of this study are available upon reasonable request from the corresponding author.

Received: 22 November 2022; Accepted: 9 June 2023;
Published online: 03 July 2023

REFERENCES

1. Turner, J. R. Intestinal mucosal barrier function in health and disease. *Nat. Rev. Immunol.* **9**, 799–809 (2009).
2. Yang, Y. et al. Within-host evolution of a gut pathobiont facilitates liver translocation. *Nature* **607**, 563–570 (2022).
3. Manfredo Vieira, S. et al. Translocation of a gut pathobiont drives autoimmunity in mice and humans. *Science* **359**, 1156–1161 (2018).
4. Ruff, W. E., Greiling, T. M. & Kriegel, M. A. Host-microbiota interactions in immune-mediated diseases. *Nat. Rev. Microbiol.* **18**, 521–538 (2020).
5. Akdis, C. A. Does the epithelial barrier hypothesis explain the increase in allergy, autoimmunity and other chronic conditions? *Nat. Rev. Immunol.* **21**, 739–751 (2021).
6. Schoultz, I. & Keita, Å. V. The intestinal barrier and current techniques for the assessment of gut permeability. *Cells* **9**, 1909 (2020).
7. Yissachar, N. et al. An intestinal organ culture system uncovers a role for the nervous system in microbe-immune crosstalk. *Cell* **168**, 1135.e12 (2017).
8. Duscha, A. et al. Propionic acid shapes the multiple sclerosis disease course by an immunomodulatory mechanism. *Cell* **180**, 1067.e16 (2020).
9. Bootz-Maoz, H. et al. Diet-induced modifications to human microbiome reshape colonic homeostasis in irritable bowel syndrome. *Cell Rep.* **41**, 111657 (2022).
10. Grosheva, I. et al. High-throughput screen identifies host and microbiota regulators of intestinal barrier function. *Gastroenterology* **159**, 1807–1823 (2020).
11. Heppert, J. K. et al. Transcriptional programmes underlying cellular identity and microbial responsiveness in the intestinal epithelium. *Nat. Rev. Gastroenterol. Hepatol.* **18**, 7–23 (2021).
12. Tilg, H., Zmora, N., Adolph, T. E. & Elinav, E. The intestinal microbiota fuelling metabolic inflammation. *Nat. Rev. Immunol.* **20**, 40–54 (2019).
13. Azriel, S., Bootz, H., Shemesh, A., Amidror, S. & Yissachar, N. An intestinal gut organ culture system for analyzing host-microbiota interactions. *J. Vis. Exp.* https://doi.org/10.3791/62779 (2021).
14. Tsai, P.-Y. et al. IL-22 upregulates epithelial Claudin-2 to drive diarrhea and enteric pathogen clearance. *Cell Host Microbe* **21**, 671.e4 (2017).
15. Elamin, E. et al. Ethanol impairs intestinal barrier function in humans through mitogen activated protein kinase signaling: a combined in vivo and in vitro approach. *PLoS ONE* **9**, e107421 (2014).
16. Tan, T. G. et al. Identifying species of symbiont bacteria from the human gut that, alone, can induce intestinal Th17 cells in mice. *Proc. Natl Acad. Sci. USA* **113**, E8141–E8150 (2016).
17. Mazmanian, S. K., Round, J. L. & Kasper, D. L. A microbial symbiosis factor prevents intestinal inflammatory disease. *Nature* **453**, 620–625 (2008).
18. Wang, H. et al. Bacteroides acidifaciens in the gut plays a protective role against CD95-mediated liver injury. *Gut Microbes* **14**, 2027853 (2022).
19. Yang, J.-Y. et al. Gut commensal Bacteroides acidifaciens prevents obesity and improves insulin sensitivity in mice. *Mucosal Immunol.* **10**, 104–116 (2017).
20. Huang, G. et al. Ginsenosides Rb3 and Rd reduce polyps formation while reinstate the dysbiotic gut microbiota and the intestinal microenvironment in ApcMin/+ mice. *Sci. Rep.* **7**, 12552 (2017).

ACKNOWLEDGEMENTS

This work is dedicated to the loving memory of Professor Nir Friedman z"l—a dear friend, a mentor, and a source of inspiration. We thank Sondra Turjeman for critical editing of the manuscript; Gitali Naim, Hagar Morad, Shir Ben-Aaron, and Nadav Vernia for computational image analysis; and members of the Yissachar lab for insightful discussions. This work was supported by the Israel Science Foundation (grant No. 1384/18), the Israel Science Foundation-Broad Institute Joint Program (grant No. 2615/18), the Israel Science Foundation-Israel Precision Medicine Partnership (grant No. 3061/22), and the Gassner Fund for Medical Research, Israel.

AUTHOR CONTRIBUTIONS

Conceptualization, S.D.M.-R., H.B.-M., S.A., E.E., and N.Y.; investigation, H.B.-M., A.S., S.D.M.-R., Y.B., D.Z., and S.A; writing, H.B.-M., A.S., and N.Y.; funding acquisition, N.Y.

COMPETING INTERESTS

The authors declare no competing interests.

ADDITIONAL INFORMATION

Supplementary information The online version contains supplementary material available at https://doi.org/10.1038/s41522-023-00409-0.

Correspondence and requests for materials should be addressed to Nissan Yissachar.

Reprints and permission information is available at http://www.nature.com/reprints

Publisher's note Springer Nature remains neutral with regard to jurisdictional claims in published maps and institutional affiliations.